Eur. Phys. J. E (2014) **37**: 94
DOI 10.1140/epje/i2014-14094-1

THE EUROPEAN PHYSICAL JOURNAL E

Regular Article

How does thermodiffusion of aqueous solutions depend on concentration and hydrophobicity?*

Kousaku Maeda[1,a], Naoki Shinyashiki[1], Shin Yagihara[1], Simone Wiegand[2,3], and Rio Kita[1,b]

[1] Graduate School of Science and Technology, Tokai University, Hiratsuka, Kanagawa 259-1292, Japan
[2] ICS-3 Soft Condensed Matter, Forschungszentrum Jülich GmbH, D-52428 Jülich, Germany
[3] Department für Chemie - Physikalische Chemie, Universität zu Köln, 50939 Cologne, Germany

Received 10 July 2014 and Received in final form 15 September 2014
Published online: 23 October 2014 –

Abstract. The thermal diffusion of aqueous solutions of mono-, di-ethylene glycols, poly(ethylene glycol), methanol, and glycerol is investigated systematically as a function of concentration using the Thermal Diffusion Forced Rayleigh Scattering (TDFRS). For all investigated binary mixtures, the Soret coefficient, S_T, decays with increasing concentration of the non-aqueous component showing two regions. For aqueous solution of ethylene glycol, at a very low solute content the decay is steep, while it becomes less steep for higher solute concentration. All mixtures show a sign change of S_T with concentration. The sign change concentration is discussed with respect to chemical structures of solute molecules and the partition coefficient, $\log p$. It turns out that the number of hydroxyl groups plays an important role. For the investigated aqueous mixtures, we find empirical linear relations between the sign change concentration and the ratio of the number of hydroxyl groups to the number of carbon atoms as well as the partition coefficient, $\log p$.

1 Introduction

A temperature gradient induces the migration of molecules in a fluid mixture. For binary mixtures, the flux of component in a temperature gradient, ∇T, in the absence of convection is written as $\mathbf{J} = -\rho D \nabla w - \rho w(1-w) D_T \nabla T$ [1]. Here, ρ is the density of the solution, D is the mutual diffusion coefficient, w is the weight fraction of component, and D_T is the thermal diffusion coefficient. The first term is well known as Fick's law. And the second term describes the thermal diffusion process, which results in the mass diffusion induced by a temperature gradient. In the steady state, $\mathbf{J} = 0$, a concentration gradient, ∇w, is formed and the ratio of D_T and D defines the Soret coefficient, S_T, as follows:

$$S_T \equiv \frac{D_T}{D} = -\frac{1}{w(1-w)} \frac{\nabla w}{\nabla T}. \tag{1}$$

In the past the thermodiffusion behavior has been investigated experimentally by various methods [2–10], by theories [11–15], and by simulations [16–19]. There are numerous thermodiffusion studies of aqueous solutions [20–25], non-aqueous mixtures [26–30], colloidal dispersions [31–36], and polymer blends [37,38]. For systems with specific interactions a sign change of S_T and D_T as functions of concentration [3,6,8,16,17,20,22,29,39–42] and temperature [5,21,43] has been often observed. For some aqueous mixtures the sign change occurs at the same concentration, where nuclear magnetic resonance (NMR) measurements indicate a breakdown of the hydrogen bond network [5,16,44]. Additionally, Polyakov and Wiegand found for some aqueous solutions a linear correlation between the ratio of the enthalpy of vaporization of the pure components and the sign change concentration [22], which is also supported by simulations of a Lennard-Jones liquid [45].

In this study, we measured the concentration dependence of S_T for aqueous solutions of ethylene glycol (EG), diethylene glycol (2EG), polyethylene glycol (13EG, 600 g/mol), methanol, and glycerol. The Thermal Diffusion Forced Rayleigh Scattering (TDFRS) is used to determine S_T and D_T. The chain length dependence is discussed using ethylene glycol oligomers (EGs), mono-, di-, and tri-alcohols. In the case of alcohols, we analyzed the relation between the thermodiffusion behavior and relate it with the number of hydroxyl groups and with the so-called partition coefficient, $\log p$ [46]. Additionally, the concentration dependence of S_T is investigated over a broad concentration range. Figure 1 shows an overview of the studied and discussed solute molecules. For instance, the concentration dependence of S_T of aqueous solutions

* Contribution to the Topical Issue "Thermal non-equilibrium phenomena in multi-component fluids" edited by Fabrizio Croccolo and Henri Bataller.

[a] e-mail: mae.kousaku@gmail.com
[b] e-mail: rkita@keyaki.cc.u-tokai.ac.jp

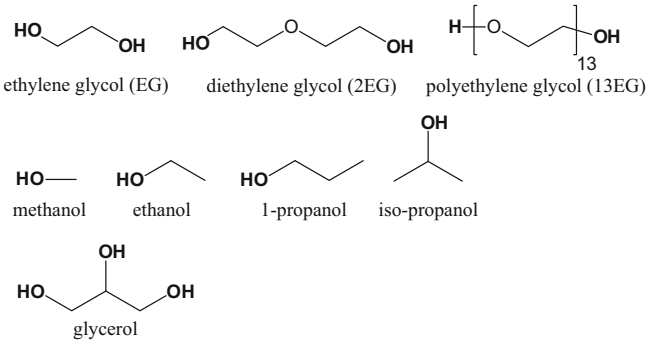

Fig. 1. The chemical structures of ethylene glycol (EG), diethylene glycol (2EG), polyethylene glycol (13EG), methanol, ethanol, 1-propanol, iso-propanol, and glycerol.

of ethanol, 1-propanol, and iso-propanol has been taken from the literature [16, 17, 39, 42]. Looking at fig. 1 it is obvious that with increasing chain length of the ethylenes and alcohols, the ratio of the number of hydroxyl groups compared to the number of carbon molecules decreases and the molecules are less hydrophilic. This coefficient is another indicator for hydrophilicity and hydrophobicity, which is also often used in the drug development [47].

2 Experimental

The compounds ethylene glycol (EG, $\geq$ 99.5%), diethylene glycol (2EG, $\geq$ 99%), poly(ethylene glycol) (13EG, 600 g/mol), methanol ($\geq$ 99.7%), and glycerol ($\geq$ 99%) were purchased at Wako chemicals. Distilled and deionized water (milli-Q) was used as a solvent. The investigated concentration range was 0.10–95.0 wt% for EG and 10.0–90.0 wt% for the other samples. All mixtures were measured at 25.0 °C. The Thermal Diffusion Forced Rayleigh Scattering (TDFRS) was used to obtain the Soret coefficient, S_T, the mutual diffusion coefficient, D, and the thermal diffusion coefficient, D_T [48,49]. The normalized heterodyne signal of the TDFRS experiment, ζ_{het}, is given by

$$\zeta_{het}(t) = 1 - \exp\left(-\frac{t}{\tau_{th}}\right) - \frac{A}{\tau - \tau_{th}} \cdot \left[\tau\left[1 - \exp\left(-\frac{t}{\tau}\right)\right] - \tau_{th}\left[1 - \exp\left(-\frac{t}{\tau_{th}}\right)\right]\right], \quad (2)$$

where, τ_{th} is the time constant of heat diffusion, τ is the time constant of the collective diffusion, and the amplitude A is given by

$$A = \frac{(\partial n/\partial w)_{p,T}}{(\partial n/\partial T)_{p,w}} S_T w(1-w). \quad (3)$$

A He-Ne laser (JDSU, 1145P, λ = 633 nm) and a solid-state laser (COHERENT, SAPPHIRE 488-200 CDRH, λ = 488 nm) were used as read and writing beams in the TDFRS setup. A little amount of dye (Basantol Yellow,

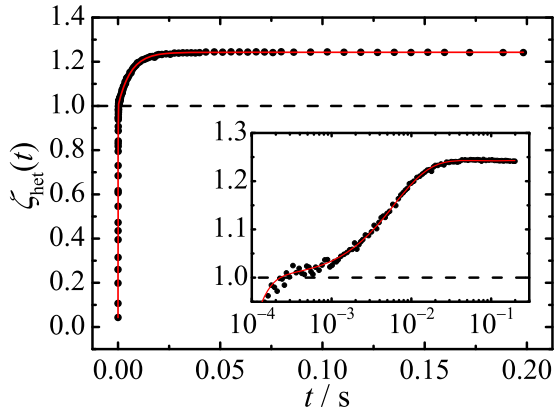

Fig. 2. The normalized heterodyne TDFRS signal for 10.0 wt% for aqueous solution of ethylene glycol (EG) measured at 25.0 °C.

$\sim$ 0.13 wt%) was added to each sample. The temperature and concentration dependences of the refractive index derivatives with temperature, $(\partial n/\partial T)_{p,w}$, and with concentration, $(\partial n/\partial w)_{p,T}$, were measured by a Michelson interferometer [50] and an Abbe refractometer (DR-M2, ATAGO) at λ = 633 nm. Figure 2 shows a typical normalized heterodyne TDFRS signal for 10.0 wt% ethylene glycol in water measured at 25.0 °C. The first process at short times is the heat diffusion and second slower process is the thermal diffusion signal of the aqueous solution of ethylene glycol. Using eqs. (2) and (3), S_T and D can be determined by the amplitude, A, with $D = 1/(q^2\tau)$ and by the equilibration time constant, τ, of the slow process. The magnitude of the scattering factor, q, can be determined from the fringe spacing of the optical grating $d = 2\pi/q$. Then, D_T is calculated using eq. (1).

3 Results and discussion

Figure 3 shows the decrease of the Soret coefficient, S_T, with increasing weight fraction of EG for an aqueous mixture. We can identify two regimes. At low weight factions w = 0.001–0.02 (dotted curve), we observe a very steep decrease, while at higher weight fractions w = 0.02–0.95 (solid curve), the slope becomes less steep. In the diluted regime, the concentration dependence of S_T is inversely proportional to w and follows the empirical equation

$$S_T(w) = \frac{a_1}{w} + b_1. \quad (4)$$

Here, a_1 and b_1 are adjustable parameters determined by a least-square curve fit. In the concentrated regime, S_T changes its sign at w = 0.65. Although the concentration dependence of S_T looks almost linear, it leads to large systematic deviations. Therefore, we used a third-order polynomial fit to describe the data. As displayed in fig. 4 also for the mutual diffusion coefficient two concentration regimes can be identified. For diluted concentrations D increases and for high concentrations D decays. The steep increase at very low concentration shows an analogy to the

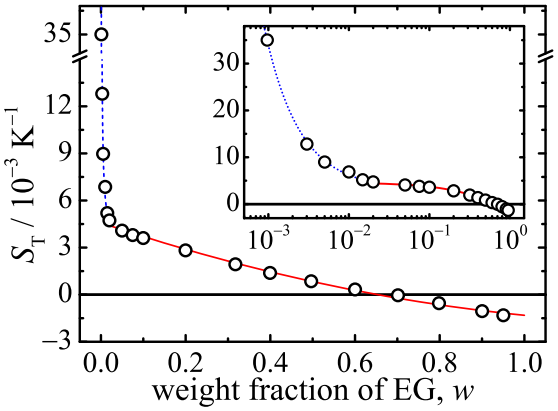

Fig. 3. The Soret coefficient, S_T, as a function of weight fraction of EG for the aqueous solution of EG. Dotted curves are drawn by $S_T = a_1/w + b_1$, and the solid curve is a third-order polynomial fit.

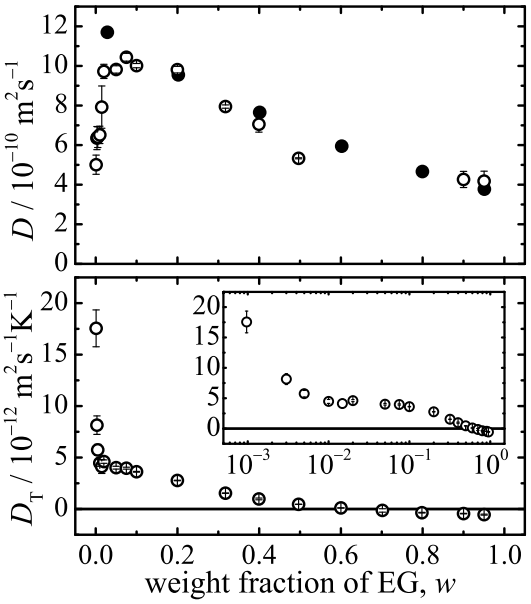

Fig. 4. The mutual diffusion coefficient, D, and the thermal diffusion coefficient, D_T, as a function of the weight fraction of EG for the aqueous mixture of EG. The solid data points are diffusion coefficient measurements by Ternstrom *et al.* [52].

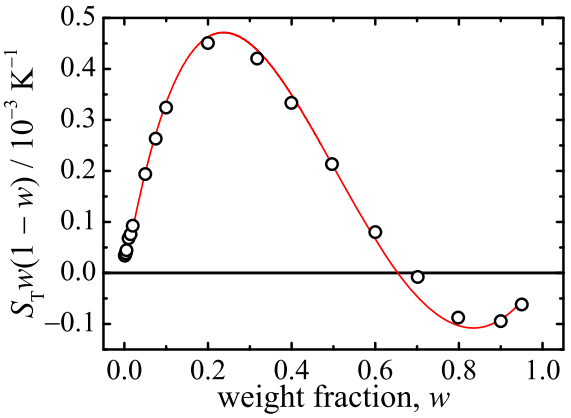

Fig. 5. $S_T w(1-w)$ as a function of weight fraction of EG for aqueous solution of EG.

well-known speeding-up of the collective diffusion within the diluted regime in polymer solutions [51]. To the best of our knowledge there is no literature for the dilute aqueous mixture. For the higher concentrations we find our data in good agreement with literature results [52]. The steep increase at very low concentrations could also be an artifact due to the small amount of Basantol Yellow which especially influences the solute concentrations, because in the Basantol Yellow the weight fraction is comparable to the solute concentration. For aqueous solutions of EG with $w = 0.003$ S_T seems to show a decrease with decreasing Basantol Yellow content, but, due to the large uncertainties of the very weak signals, we were not able to quantify the effect. To clarify the dye concentration effect, future experiments with IR-TDFRS [49] or the beam deflection method [53] would be useful.

The established concentration gradient, ∇w, is characterized by S_T, and can be written as $\nabla w/\nabla T = -S_T w(1-w)$ according to eq. (1). Figure 5 displays $S_T w(1-w)$ as a function of the weight fraction of EG for the aqueous mixture. We observe a maximum and a minimum at $w = 0.24$ and 0.83, respectively. At the peak concentrations, the mixture shows the highest separation efficiency, and the EG molecules accumulate at the cold and hot side at $w = 0.24$ and 0.83, respectively. $S_T w(1-w)$ approaches zero at the low and high concentration limits. However, due to the fact that S_T is inversely proportional to the weight fraction in the low concentration regime, S_T has to converge to a finite value [51,54]. Due to the symmetry argument we expect also in the high concentration limit a finite value when the steep decrease of S_T at low concentration is not caused by the dye.

The sign change occurs at a weight fraction of $w^{\pm} = 0.65$ corresponding to a mole fraction of $x^{\pm} = 0.39$. Previously, the molar sign change concentration, $x^{\pm}$, has been obtained for various aqueous solutions [16,22,39,42]. The mole fraction $x^{\pm}$ of acetone, DMSO, ethanol, and propionaldehyde could be linearly related to the ratio of the vaporization of the pure components for aqueous solutions [22]. The common nature of the compounds following this trend seems to be two non-polar carbons connected by a single bond and one oxygen atom. The sign change mole fraction of EG is too high as in the case of methanol and does not follow the same trend. Compared to the solute molecules following the trend EG and methanol are more polar. The other class of systems not following the trend has a too low sign change concentration and is too non-polar.

Figure 6 shows S_T as a function of weight and mole fraction of the solute molecule for aqueous solutions of methanol, ethanol [39], 1-propanol [22], iso-propanol [42] (top), EG, 2EG, 13EG (middle), and glycerol (bottom). All aqueous solutions show a sign change with concentration. At low concentration, all solute molecules (alcohols or EGs) migrate to the cold side, while at high concentration, the solvent molecule (water) migrates to the cold

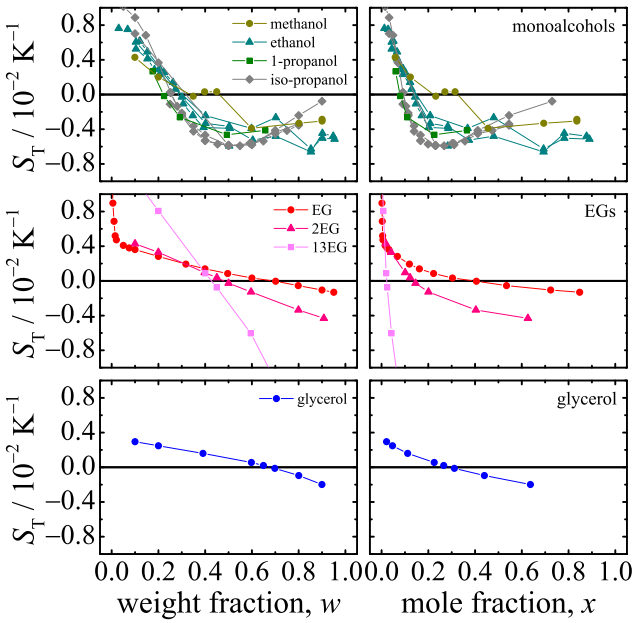

Fig. 6. The Soret coefficient, S_T, as a function of the weight fraction (left) and the mole fraction (right) of aqueous solutions of monoalcohols, EGs, and glycerol at 25 °C.

side. This finding agrees with other experimental studies [16] and simulations [55] and is related to the strong cross interactions in polar mixtures [56, 57]. If the cross interaction of the two components is stronger than the average values of the pure components, the minority component accumulates always on the cold side.

Further we noticed that the weight fraction $w^{\pm}$ increases with increasing number of hydroxyl groups, N_{OH}. The concentrations $w^{\pm}$ and $x^{\pm}$ decrease with increasing the number of carbon atoms, N_C, for monoalcohols and EGs. The molar sign change concentration, $x^{\pm}$, is inversely proportional to N_C. Figure 7 shows $w^{\pm}$ and $x^{\pm}$ as a function of the number of carbon atoms, N_C, for all solute molecules. Curves are fitted to a function inversely proportional to N_C plus a baseline. The sign change concentrations $w^{\pm}$ and $x^{\pm}$ decrease with increasing N_C. The mole fraction $x^{\pm}$ is proportional to N_{OH} and the ratio of N_{OH} to N_C,

$$x^{\pm}(N_{OH}, N_C) = \alpha \frac{N_{OH}}{N_C} . \qquad (5)$$

Here, α is a factor, $\alpha = 0.278 \pm 0.006$. Figure 8 shows $x^{\pm}$ as a function of N_{OH}/N_C. The line is a linear fit according to eq. (5). All data except for EG follow a single master curve. This indicates that the sign change concentration becomes higher if the solute molecule is more hydrophilic and more compatible with water. This is the case, if the number of hydroxyl groups increases, which work as a donor of hydrogen bonding. Figure 9 shows the weight sign change concentration, $w^{\pm}$, as a function of logarithm of the partition coefficient between n-octanol and water, $\log p$ [46, 58]. Log p values were calculated by ChemAxon Marvin. The sign change concentration depends linearly on $\log p$ and the hydrophobic molecules show a smaller $x^{\pm}$

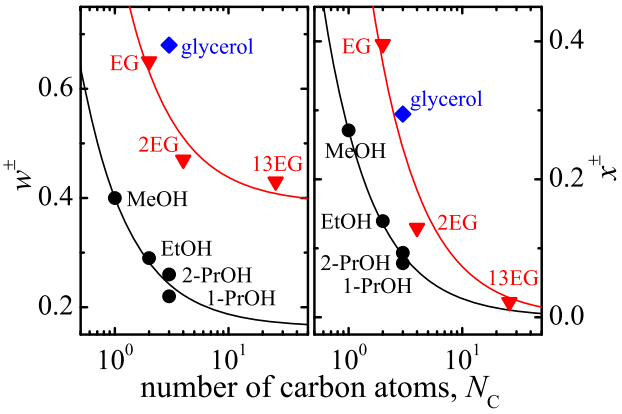

Fig. 7. The weight and molar sign change concentrations, $w^{\pm}$ and $x^{\pm}$, as a function of the number of carbon atoms, N_C, in each molecule. The solid curves are fitted to a function inversely proportional to N_C plus a baseline.

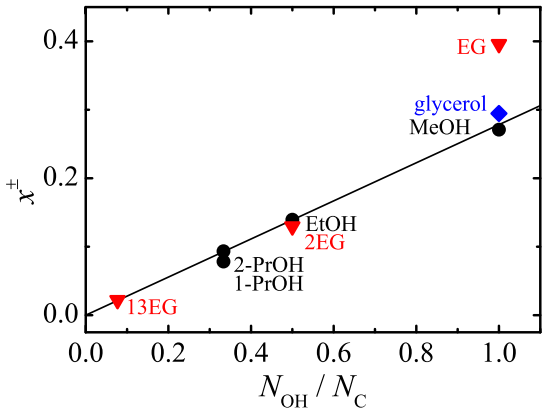

Fig. 8. The molar sign change concentration, $x^{\pm}$, as a function of N_{OH}/N_C.

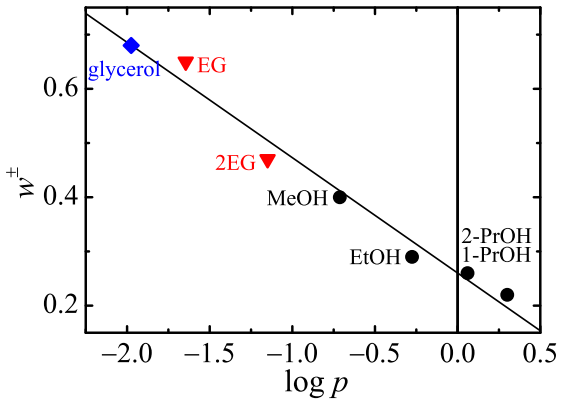

Fig. 9. The weight sign change concentration, $w^{\pm}$, as a function of the logarithm of the partition coefficient between n-octanol and water, $\log p$.

compared to the hydrophilic molecules. We assume that in the case of hydrophobic solute molecules, the breakdown of the hydrogen bond network occurs at lower concentrations and leads them to a sign change, as observed for 1-propanol and iso-propanol in fig. 9.

Table 1. The list of the Soret coefficient, S_T, the sign change concentrations $w^{\pm}$, $x^{\pm}$, and the partition coefficient, $\log p$, for equimolar aqueous mixtures.

Sample	$S_T/10^{-3}\,K^{-1}$	$w^{\pm}$	$x^{\pm}$	$\log p$
EG	−0.41	0.65	0.39	−1.645
2EG	−4	0.47	0.13	−1.15
Glycerol	−1.2	0.68	0.29	−1.975
Methanol	−3.5	0.40	0.27	−0.713
Ethanol [39]	−4	0.29	0.14	−0.276
1-propanol [22]	−3.5[(a)]	0.22	0.08	0.3
Iso-propanol [42]	−4.0	0.26	0.09	0.06
DMSO [22]	−2.96	0.55	0.22	
Acetone [16]	−17.0	0.28	0.11	
13EG	−22[(a)]	0.43	0.02	

[(a)] Extrapolation values of measurement results.

All molar sign change concentrations, $x^{\pm}$, considered in this study are below $x^{\pm} = 0.5$. Therefore it follows that S_T for all solute molecules is negative for equimolar mixtures. Hartmann *et al*. reported the thermal diffusion for binary equimolar mixtures of ten different solvents [9]. The Soret coefficient, S_T, of nine solute molecules dissolved in hexane is positive and S_T of eight solute molecules dissolved in cis-decalin is negative. Hexane is very thermophilic, so that it migrates to the hot side, while the dissolved solute molecules accumulate at the cold side. Cis-decalin is thermophobic, and it migrates to the cold side. Following this argumentation, water behaves like a thermophobic molecule at $x = 0.5$. Table 1 shows S_T, $w^{\pm}$, $x^{\pm}$, and $\log p$ of the discussed solute molecules in water for equimolar mixtures. The Soret coefficient, S_T, of 13EG has the lowest value, which is caused by the hydrophobic character of 13EG, which leads also to a low $x^{\pm}$. S_T for most aqueous solutions decays monotonically with concentration, except for 1-propanol, iso-propanol, and acetone, which show an increase of S_T at higher solute concentrations [16, 22, 42], therefore, S_T of equimolar mixtures decreases typically with decreasing $x^{\pm}$.

A direct comparison with the results of Hartmann *et al.* [9] is not possible, because the majority of their investigated substances are non-polar solvents. Among their solvents only acetone is miscible with water. For an equimolar mixture of acetone and water $S_T = -17.0 \times 10^{-3}\,K^{-1}$ (cf. table 1), the determined heat of transport is equal to $Q_i = -3.7\,kJ/mol$ [9]. Similar Soret coefficients $S_T = -23.9 \times 10^{-3}\,K^{-1}$ and $S_T = -8.3 \times 10^{-3}\,K^{-1}$ have been measured for acetone in trans-decalin and tetralin, respectively. The average value of those two agrees almost with the measured value of acetone in water, therefore we assume, due to the almost linear dependence of S_T and Q_i, that the heat of transport of water is expected to lie between the values of the heats of transport for trans-decalin ($-1.1\,kJ/mol$) and tetralin ($0\,kJ/mol$).

4 Conclusion

In this paper we studied the thermodiffusion behavior of aqueous solutions of monoalcohols (methanol and ethanol), ethylene glycol oligomers (EG, 2EG, and 13EG) and glycerol. The selected solute molecules varied systematically in their chemical structure. It turned out that especially the ratio of the number of hydroxyl groups to carbon atoms, N_{OH}/N_C, is a crucial parameter. For all studied systems we observed a sign change of S_T with concentration and it turns out that with increasing hydrophilicity the sign change concentration increases, indicating that the hydrogen bond network gets more easily destroyed at lower concentrations, if the molecules become more hydrophobic. This correlation between the sign change concentration and the destruction of the hydrogen bond network has been reported before [5, 16]. We quantified the hydrophilicity of the system by two parameters: the ratio of number of hydroxyl groups to carbon atoms, N_{OH}/N_C, and the partition coefficient, $\log p$. It turned out that the determined molar sign change concentration, $x^{\pm}$, showed a clear linear correlation with the ratio of number of hydroxyl groups to carbon atoms, N_{OH}/N_C. Additionally, the weight sign change concentration, $w^{\pm}$, varied linearly with the partition coefficient, $\log p$. Both parameters are easily accessible and might be used in future studies to select systems and measurements ranges with thermophilic and thermophobic behavior.

This work is partially supported by KAKENHI (No. 24350122 and No. 26103529 "Fluctuation & Structure") from MEXT, Japan. Partial financial support due to the Deutsche Forschungsgemeinschaft grant Wi 1684 is gratefully acknowledged.

References

1. S. de Groot, P. Mazur, *Non-Equilibrium Thermodynamics* (Dover, New York, 1984).
2. M. Bou-Ali, O. Ecenarro, J. Madariaga, C. Santamaria, J. Non-Equilib. Thermodyn. **24**, 228 (1999).
3. C. Debuschewitz, W. Köhler, Phys. Rev. Lett. **87**, 055901 (2001).
4. J. Chan, J. Popov, S. Kolisnek-Kehl, D. Leaist, J. Sol. Chem. **32**, 197 (2003).
5. R. Kita, S. Wiegand, J. Luettmer-Strathmann, J. Chem. Phys. **121**, 3874 (2004).
6. G. Wittko, W. Köhler, EPL **78**, 46007 (2007).
7. P. Blanco, P. Polyakov, M. Bou-Ali, S. Wiegand, J. Phys. Chem. B **112**, 8340 (2008).
8. A. Königer, B. Meier, W. Köhler, Philos. Mag. **89**, 907 (2009).
9. S. Hartmann, G. Wittko, W. Köhler, K. Morozov, K. Albers, G. Sadowski, Phys. Rev. Lett. **109**, 065901 (2012).
10. F. Croccolo, H. Bataller, F. Scheffold, J. Chem. Phys. **137**, 234202 (2012).
11. J. Luettmer-Strathmann, J. Chem. Phys. **119**, 2892 (2003).

12. S. Pan, C. Jiang, Y. Yan, M. Kawaji, M. Saghir, J. Non-Equilib. Thermodyn. **31**, 47 (2006).
13. S. Pan, M. Saghir, M. Kawaji, C. Jiang, Y. Yan, J. Chem. Phys. **126**, 014502 (2007).
14. A. Würger, Rep. Prog. Phys. **73**, 126601 (2010).
15. A. Würger, J. Phys.: Condens. Matter **26**, 035105 (2014).
16. H. Ning, S. Wiegand, J. Chem. Phys. **125**, 221102 (2006).
17. P. Polyakov, M. Zhang, F. Müller-Plathe, S. Wiegand, J. Chem. Phys. **127**, 014502 (2007).
18. C. Jiang, T. Jaber, H. Bataller, M. Saghir, Int. J. Therm. Sci. **47**, 126 (2008).
19. A. Abbasi, M. Saghir, M. Kawaji, Int. J. Therm. Sci. **50**, 124 (2011).
20. B. de Gans, R. Kita, S. Wiegand, J. Luettmer-Strathmann, Phys. Rev. Lett. **91**, 245501 (2003).
21. R. Sugaya, B. Wolf, R. Kita, Biomacromolecules **7**, 435 (2006).
22. P. Polyakov, S. Wiegand, J. Chem. Phys. **128**, 034505 (2008).
23. P. Blanco, H. Kriegs, B. Arlt, S. Wiegand, J. Phys. Chem. B **114**, 10740 (2010).
24. P. Blanco, S. Wiegand, J. Phys. Chem. B **114**, 2807 (2010).
25. Y. Kishikawa, S. Wiegand, R. Kita, Biomacromolecules **11**, 740 (2010).
26. K. Zhang, M. Briggs, R. Gammon, J. Sengers, J. Douglas, J. Chem. Phys. **111**, 2270 (1999).
27. J. Platten, M.M. Bou-Ali, P. Costeseque, J. Dutrieux, W. Köhler, C. Leppla, S. Wiegand, G. Wittko, Philos. Mag. **83**, 1965 (2003).
28. G. Wittko, W. Köhler, J. Chem. Phys. **123**, 014506 (2005).
29. P. Polyakov, J. Luettmer-Strathmann, S. Wiegand, J. Phys. Chem. B **110**, 26215 (2006).
30. M. Hartung, W. Köhler, Rev. Sci. Instrum. **78**, 084901 (2007).
31. R. Piazza, A. Guarino, Phys. Rev. Lett. **88**, 208302 (2002).
32. R. Piazza, Philos. Mag. **83**, 2067 (2003).
33. A. Würger, Phys. Rev. Lett. **101**, 108302 (2008).
34. A. Würger, Langmuir **25**, 6696 (2009).
35. A. Königer, N. Plack, W. Köhler, M. Siebenburger, M. Ballauff, Soft Matter **9**, 1418 (2013).
36. Z. Wang, H. Kriegs, J. Buitenhuis, J. Dhont, S. Wiegand, Soft Matter **9**, 8697 (2013).
37. W. Enge, W. Köhler, Chem. Phys. Chem. **5**, 393 (2004).
38. W. Köhler, A. Krekhov, W. Zimmermann, Adv. Polym. Sci. **227**, 145 (2010).
39. P. Kolodner, H. Williams, C. Moe, J. Chem. Phys. **88**, 6512 (1988).
40. G. Wittko, W. Köhler, Eur. Phys. J. E **21**, 283 (2006).
41. S. Hartmann, W. Köhler, K. Morozov, Soft Matter **8**, 1355 (2012).
42. A. Mialdun, V. Yasnou, V. Shevtsova, A. Königer, W. Köhler, D. de Mezquia, M. Bou-Ali, J. Chem. Phys. **136**, 244512 (2012).
43. S. Iacopini, R. Piazza, Europhys. Lett. **63**, 247 (2003).
44. A. Coccia, P. Indovina, F. Podo, V. Viti, Chem. Phys. **7**, 30 (1975).
45. D. Reith, F. Müller-Plathe, J. Chem. Phys. **112**, 2436 (2000).
46. G. Klopman, J. Li, S. Wang, M. Dimayuga, J. Chem. Inf. Comput. Sci. **34**, 752 (1994).
47. C. Lipinski, F. Lombardo, B. Dominy, P. Feeney, Adv. Drug Deliv. Rev. **64**, 4 (2012).
48. S. Wiegand, J. Phys.: Condens. Matter **16**, R357 (2004).
49. S. Wiegand, H. Ning, H. Kriegs, J. Phys. Chem. B **111**, 14169 (2007).
50. G. Wittko, W. Köhler, Philos. Mag. **83**, 1973 (2003).
51. J. Rauch, W. Köhler, J. Chem. Phys. **119**, 11977 (2003).
52. G. Ternström, A. Sjöstrand, G. Aly, A. Jernqvist, J. Chem. Eng. Data **41**, 876 (1996).
53. D. Vigolo, G. Brambilla, R. Piazza, Phys. Rev. E **75**, 040401 (2007).
54. J. Rauch, W. Köhler, Phys. Rev. Lett.. **88**, 185901 (2002).
55. B. Rousseau, C. Nieto-Draghi, J. Avalos, Europhys. Lett. **67**, 976 (2004).
56. I. Prigogine, L. Debrouckere, R. Amand, Physica **16**, 577 (1950).
57. I. Prigogine, L. Debrouckere, R. Amand, Physica **16**, 851 (1950).
58. Z. Wang, H. Kriegs, S. Wiegand, J. Phys. Chem. B **116**, 7463 (2012).